Available online at www.sciencedirect.com
ScienceDirect
Biochimica et Biophysica Acta 1768 (2007) 236–245
Biochimica et Biophysica Acta
BBA
www.elsevier.com/locate/bbamem

Defect formation of lytic peptides in lipid membranes and their influence on the thermodynamic properties of the pore environment

Vitaliy Oliynyk [a,b], Udo Kaatze [a], Thomas Heimburg [b,*]

[a] Complex Fluids Group, Drittes Physikalisches Institut, Georg-August Universität, Friedrich-Hund-Platz 1, D-37077 Göttingen, Germany
[b] Membrane Biophysics Group, Niels Bohr Institut, University of Copenhagen, Blegdamsvej 17, DK-2100 Copenhagen Ø, Denmark

Received 31 May 2006; received in revised form 10 October 2006; accepted 11 October 2006
Available online 24 October 2006

Abstract

We present an experimental study of the pore formation processes of small amphipathic peptides in model phosphocholine lipid membranes. We used atomic force microscopy to characterize the spatial organization and structure of alamethicin- and melittin-induced defects in lipid bilayer membranes and the influence of the peptide on local membrane properties. Alamethicin induced holes in gel DPPC membranes were directly visualized at different peptide concentrations. We found that the thermodynamic state of lipids in gel membranes can be influenced by the presence of alamethicin such that nanoscopic domains of fluid lipids form close to the peptide pores, and that the elastic constants of the membrane are altered in their vicinity. Melittin-induced holes were visualized in DPPC and DLPC membranes at room temperature in order to study the influence of the membrane state on the peptide induced hole formation. Also differential scanning calorimetry was used to investigate the effect of alamethicin on the lipid membrane phase behaviour.

Keywords: Peptide pores; Lipid membranes; Alamethicin; Melittin; Atomic force microscopy; Differential scanning calorimetry

1. Introduction

The biological activities of membrane active peptides are determined to a large part by their interactions with the phospholipid bilayer comprising the plasma membrane and the mutual structural effects induced within the peptide and lipid molecules. Many native and synthetic peptides are known to, under certain conditions, form spontaneously transmembrane defects, such as pores, in lipid bilayers. Defect formation is promoted by a combination of electrostatic interactions of the peptide residues with the polar heads of anionic lipid molecules and hydrophobic interactions with the lipid acyl chains [1–3]. It is commonly believed that the defect formation is the mode of action of antimicrobial peptides. These peptides are active, forming pores, in some cell membranes but not in others, such that they can function as host-defense agents, killing microbes. On certain conditions, however, they are just associated to the membrane surface where they are inactive. Studies of defect formation and of the defect structures in lipid bilayers may be a key step toward our understanding of how the activities of antimicrobial peptides are regulated in the biological world.

Amphipathic, α-helical peptides are abundant in nature, serving as membrane permeating agents in the host defense system of many organisms. Antibiotic peptides, such as alamethicin, isolated from the *Trichoderma viride fungus*, and the bee venom peptide melittin are among the most intensively studied peptides [4,5]. As the amino-acid sequence and the helical structure in water as well as membrane environments of these peptides is well known, they can serve as convenient models for studies of interactions between membrane located proteins and lipids. The crystal structures of alamethicin and melittin have been solved more than twenty years ago by X-ray crystallography [6–8]. At low peptide-to-lipid molar ratios alamethicin preferentially adsorbs to the membrane surface where it is arranged parallel to the lipid headgroups and associated to the bilayer surface. With increasing peptide concentration, alamethicin switches to an active state. It is then inserted into the lipid membrane, forming transmembrane pores [9,10]. Above a certain critical concentration nearly all peptide

* Corresponding author. Tel.: +45 35 32 53 89; fax: +45 35 32 50 16.
E-mail address: theimbu@nbi.dk (T. Heimburg).

0005-2736/$ - see front matter © 2006 Elsevier B.V. All rights reserved.
doi:10.1016/j.bbamem.2006.10.007

molecules are participating in the pore formation process [11,12]. The structure of alamethicin channels is generally considered in terms of the "barrel-stave" model [13–17], in which multiple peptide molecules form a helix bundle surrounding a central pore. This model is capable to explain the occurrence of channel activity in discrete, multilevel conductance steps [18–21] which is caused by a varying number of pore-forming peptides. Nevertheless, in spite of the fact that a large body of experimental data was generated, the microscopic structure of alamethicin pores and the organization of peptide pores in lipid membranes is not completely understood presently.

Proteins and peptides inserted into membranes may influence the chain melting transition of lipid membranes. It is known from calorimetric studies that gel-to-fluid transition profiles are broadened and/or shifted to either lower or higher temperatures by addition of proteins [22,21–24]. The shape of the heat capacity profiles contains valuable information on the modes of interactions between peptides and lipids [22,25], for example, about their spatial organization. It has been shown that the effect of integral peptides on the phase behaviour of lipid membranes strongly depends on the chain length of the lipids [26]. This finding is discussed in terms of "hydrophobic mismatch", which implies that the interaction between integral proteins (or amphipathic peptides) and lipids depends on the relative length difference of their hydrophobic cores. It has been proposed that the hydrophobic mismatching controls the peptide partitioning in lipid membranes via lipid mediated forces [27,28].

Atomic force microscopy [29–32,41] is extensively used in recent studies for the characterization of lipid membrane systems with resolution on the nanoscopic scale. This method was successfully applied to investigate, with high spatial resolution, the structure of pure lipid membranes as well as peptide containing membranes under different conditions [33–37]. Direct visualization of peptide aggregates in model membranes as well as the study of their structure and their effect on lipid bilayers was reported for a number of native [23,38] and synthetic peptides [24,36]. The experiments reported in this study focus on the characteristics of alamethicin as well as melittin association and aggregation within lipid membranes. We found the appearance of pores or defects in the membrane induced by such peptides. We loosely refer to these features as 'defects' although they may be closely related or indistinguishable from pores. The investigation demonstrates that the structure of alamethicin- and melittin-induced transmembrane defects in gel membranes can be directly visualized for different peptide concentrations. The influence of the peptides on the phase behaviour of phosphocholine membranes is also reported. In particular, we show that the physical behaviour of the lipid membrane is altered in the vicinity of the pores.

2. Materials and methods

1,2-dipalmitoyl-*sn*-glycero-3-phosphatidylcholine (DPPC), 1,2-dimyristoyl-*sn*-glycero-3-phosphatidylcholine (DMPC) and 1,2-dilauroyl-*sn*-glycero-3-phosphocholine (DLPC) were purchased from Avanti Polar Lipids (Alabaster, AL). Alamethicin was provided by Sigma (St. Louis, MO) and melittin as a powder from Alexis Biochemicals (San Diego, CA). All substances were used without further purification. Ruby muscovite mica was obtained from TED PELLA, inc. (Redding, CA).

For the preparation of lipid–peptide multilamellar vesicle dispersions, lipids and peptides were separately dissolved in a 1:1 mixture of dichloromethane and methanol. The dissolving of lipids and peptides in the organic solvents, preceding the preparation of aqueous solutions, was required for more exact weighing of the substances in micrograms amounts and for better mixing of peptides and lipids. Further, appropriate amounts of the solutions of the target substances were mixed together, dried under a weak flow of nitrogen gas, and placed under vacuum overnight to remove the residual solvent. The dried peptide/lipid mixtures were dispersed in Milli-Q water to a final concentration of 1–3 mM. Aqueous multilamellar vesicle dispersions were prepared by heating the samples above 50 °C, followed by vortexing.

Differential scanning calorimetry (DSC) experiments [39] were performed using large unilamellar lipid vesicle (LUV) suspensions. LUVs were obtained with the aid of a small volume extrusion apparatus [40] provided by Avestin (Ottawa, Canada). The multilamellar vesicles were extruded through polycarbonate filters with 100 nm pores size, mounted in the mini-extruder and fitted with two 1.0 ml syringes. Samples were 21 times passed through the filter membrane. An odd number of passages was performed to avoid contamination of the sample by multilamellar vesicles which might not have passed through the filter. During the extrusion process the temperature of the sample was kept above the melting point of the lipids that facilitates the pushing of the lipid suspension through the filter. Right before the filling of the calorimeter the solution of extruded vesicles was degassed for 15 min in order to remove air microbubbles. DSC experiments were performed using a VP-DSC from MicroCal (Northhampton, MA) on samples of 5 mM lipid LUVs at a scan rate of 2 °C/h. An appropriate baseline was subtracted from the resulting thermograms.

Samples for atomic force microscopy (AFM) experiments [41] were prepared utilizing direct fusion of small unilamellar vesicles (SUVs) on mica [42]. Lipid SUVs were prepared in the presence of the peptides by sonication with the aid of a Sonifier Cell Disruptor B-15 (Branson, Germany) until the solution became completely transparent. Transparency ensures that the solution consists mostly of small unilamellar vesicles. The SUVs were immediately rewarmed to temperature above 55 °C, and 40–80 μl of the vesicle suspension was added to a piece of freshly cleaved mica. The samples were incubated for 20 min at room temperature and rinsed by exchanging ten times the incubation solution with 150 mM NaCl solution afterwards (rinsing by Milli-Q water was found to be also effective). In doing so the supported lipid membrane was never allowed to dry. The mica-supported lipid bilayers were imaged in both contact and tapping mode using a MultiMode atomic force microscope with NanoScope IIIa controller (Digital Instruments, Santa-Barbara, CA). Oxide-sharpened silicon nitride AFM probes (Digital Instruments, Santa-Barbara, CA) with nominal spring constants of 0.06 N/m and 0.12 N/m were used. To ensure that the force was kept minimal during scanning, the force was frequently decreased until the tip left the surface and was subsequently slightly increased until just regaining contact. The scan rate was 5–8 lines per second (Hz) for contact mode images and 1–3 lines per second (Hz) for tapping mode images. All images have 512 × 512 pixels. Analysis of AFM images was performed with non-commercial software WSxM© (Nanotec Electrónica, http://www.nanotec.es).

Here, we also present phase images obtained in tapping mode. Larger phase shifts close to peptide-generated defects were attributed to a larger softness of the membranes. However, it should be noted that currently no simple relation between phase images and the material properties is known. Larger phase shifts usually correspond to softer material, but other origins of phase shifts cannot been ruled out completely, for instance contributions from the adhesion of the membranes to the surface or the cantilever tip. The images presented here were recorded in water, meaning that there is no capillary adhesion caused by a water layer of the cantilever in air. Molecular interactions between the tip surface and lipids should be the same independent of the distance from the defects. If adhesion to the mica contributes to the phase shift, it should be the same at all parts of the sample. We found that the membranes close edges of peptide-generated defects display larger phase shifts than membrane regions further away from the defects. This was not the case for the defects found in the absence of peptides. Therefore we attributed these larger phase shifts to a change in the viscoelastic properties of the lipid membrane close to the proteins.

3. Results

3.1. Atomic force microscopy

Without membrane active peptides, mica-supported lipid bilayers in gel or fluid phases display a very flat surface when visualized with AFM resolutions. Rare structures can show up that are caused by defects in the crystal structure of the mica and by contamination or partial fusion of lipid bilayers. A random example indicating different modes of lipid membrane fusion on mica is shown in Fig. 1. Part A of this figure presents an AFM height image of a DPPC membrane supported on mica. Very dark regions of the image indicate the height level of the mica support. Hence they reveal parts of mica which were not covered by lipid. Such defects may be due either to a too short incubation time or to a too low lipid concentration in the droplet of DPPC sample placed on the freshly cleaved mica surface. Very bright areas show small pieces of a second lipid bilayer laying on the top of the first one. This view is supported by the height profile shown in part B of Fig. 1. The height of the first DPPC bilayer in the gel phase is between 5 and 6 nm which is in accordance with the accepted thickness of DPPC membranes [37]. The distance between the upper surfaces of the first and the second bilayers is by about 2 nm larger, demonstrating that it involves the thickness of a water layer between both membranes [43,44].

Parts C and E of Fig. 1 present a height image and a phase image, respectively, of the same area of a mica supported DLPC membrane. Contrary to DPPC, with main phase transition temperature T_m=41.6 °C, the DLPC membrane (T_m=−2.1 °C) is in the fluid phase at room temperature. The DLPC bilayer appears as a flat leaflet in the height image. The height profile (D, Fig. 1) indicates a membrane thickness of somewhat less than 6 nm, as determined from the height difference between the bilayer surface and the mica support surface at a membrane defect.

In the phase image of the DLPC membrane area (E, Fig. 1), which has been recorded simultaneously with the tapping mode height image, brighter colouring indicates larger phase shifts. Hence the image shows larger phase shifts in the tapping oscillations when probing the soft membrane instead of the stiff mica support. Here, phase imaging techniques will be used to highlight lateral membrane structures, in particular to study the effect of peptides upon the lateral distribution of viscoelastic membrane properties.

When 1 mol% of alamethicin is incorporated into a DPPC bilayer the surface of the membrane appears evenly perturbed in the AFM height images. As shown by parts A and D of Fig. 2 where results for two different sample preparations are presented, predominantly circularly shaped transmembrane defects result. Some elongated defects exhibit smooth round kinks, as will be discussed with more details below (dark areas in Fig. 2A, D). We assume these defects to indicate alamethicin induced membrane holes, filled with water. We were also able to directly observe melittin induced hole formation in phosphocholine lipid bilayers. Samples of DPPC and DLPC were

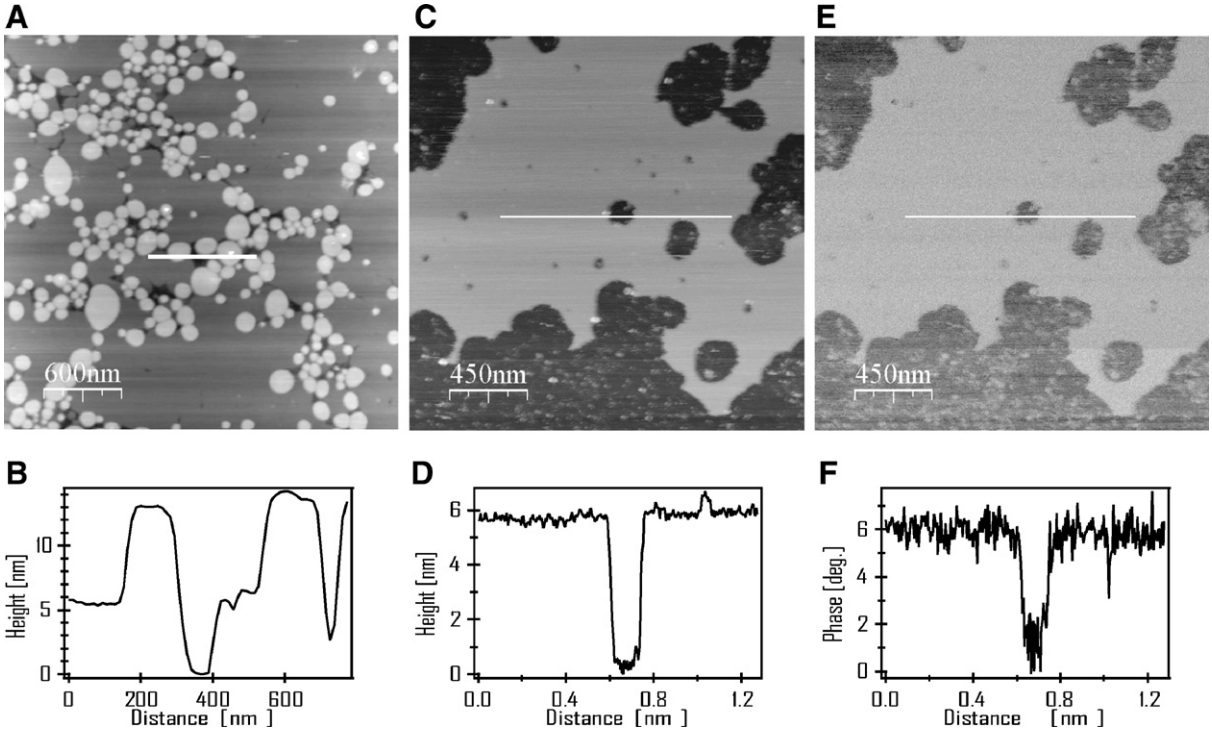

Fig. 1. Supported bilayers of DPPC and DLPC supported by mica in the absence of peptides. (A) 3×3 μm scan size height image of DPPC membrane obtained operating the AFM in contact mode and (B) cross-section plot along the white line on the height image (A), from which thicknesses of the first and the second bilayers are ~6 nm and ~8 nm. Simultaneously recorded tapping mode height (C) and phase (E) images of a DLPC membrane with 2.2×2.2 μm scan sizes where white lines mark the position of cross-section profiles shown in (D) and (F), respectively, and corresponds to the same scan line and the same position on the sample surface. All images have 512 scan lines and 512 points per line.

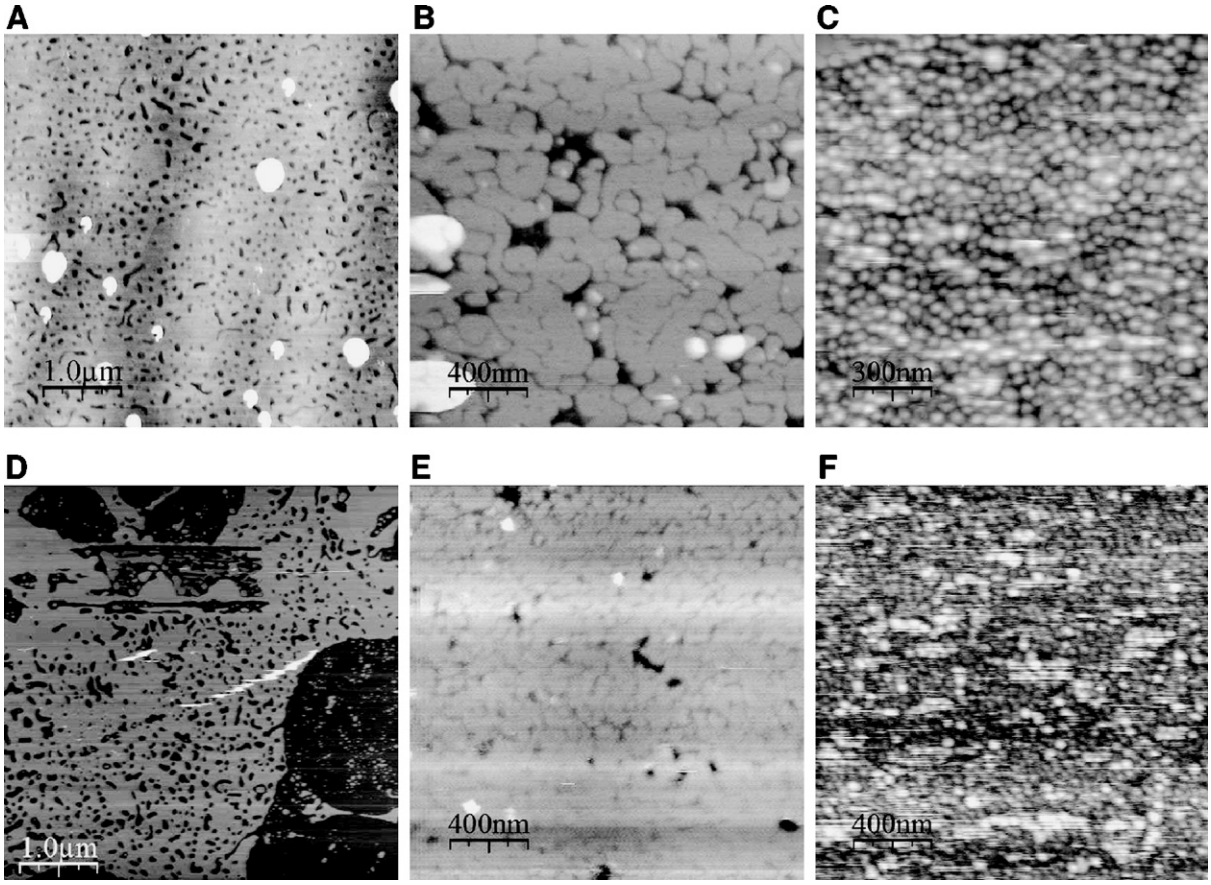

Fig. 2. Atomic force micrographs of lipid membranes deposited on mica in the presence of pore forming peptides. (A) Height image (5 × 5 μm scan size) of 1 mol% alamethicin in DPPC membranes in the gel state at 25–30 °C. Dark spots on the brighter surface of the DPPC membrane represent the mica surface, which is accessible for AFM tip via alamethicin induced transmembrane defects. White regions in all images correspond to the second sheet of lipid membrane which lies on the top of the first one. The height of the DPPC membrane slightly varies across the image, which is caused by imperfectly adjusted scanning parameters. (B) Height image (2 × 2 μm scan size) of 1 mol% melittin in DPPC membrane in the gel state. Dark regions represent the mica surface, and the bright regions represent DPPC membrane segments. Line-like depressions in the membrane can be seen. (C) Height image (1.5 × 1.5 μm scan size) of 1 mol% melittin in DLPC membrane in the fluid state. A highly developed net of depressions on the membrane surface is clearly demonstrated. The set of figures in the bottom panel (D, E and F) represents images obtained under the same conditions and for the same lipid/peptide systems as shown above (for A, B and C, respectively) but from completely different sample preparation.

investigated between 25 °C and 30 °C, both with and without 1 mol% of melittin added. Two different lipids were used, because the AFM was not provided with a sufficiently stable temperature control. The temperature of measurements was, therefore, slightly above 25 °C for both lipids. DPPC at those temperatures is in gel phase, whereas DLPC is in fluid phase. Some representative results are again shown for two different samples in parts B, E as well as C, F, respectively, of Fig. 2.

In contrast to the alamethicin, melittin forms in gel and fluid lipid bilayers (DPPC and DLPC, respectively) a widespread net of prolongated transmembrane defects with close spacing of defects sides. Already at such small amount of peptide the bilayer looks disintegrated. As another noticeable result, the pattern of melittin induced holes in DPPC and DLPC bilayers is strikingly different. In the fluid phase DLPC bilayer melittin develops a net of transmembrane defects of high density and displays a more disordered structure than in the gel phase DPPC bilayer, containing the same amount of peptide.

When the samples of DPPC bilayers containing 1 mol% of alamethicin shown in Fig. 2A was scanned on a large scale, an interesting defect structure emerged (Fig. 3A). In this image the diversity of defect formation by alamethicin is demonstrated in details. Most holes appear preferentially as round transmembrane defects of different sizes. There is also a small number of peptide induced elongated holes, some of which appear as roundish kinks of specific radius. Another interesting feature of alamethicin induced defects exists at the membrane–hole interface. Close to almost all peptide induced holes there exist kinds of shells, exhibiting a lower height (darker areas in the height images) than the undisturbed bilayer. From the height profile across one of the holes (Fig. 3C) we found the height of the shell in the range of 3 to 4 nm, whereas the bilayer thickness amounts to 5–6 nm. This feature appears in all alamethicin-containing samples independent of scan direction. It does not show up at the interface of pure lipid membranes as shown in Fig. 1. We therefore concluded that these regions at the pore interfaces are no experimental artifacts but rather a result of the interaction of the peptides with the lipid membrane in its environment. As mentioned before, the latter bilayer height is in good agreement with literature values for the thickness of gel phase DPPC lipid bilayers [45–47]. As the melting temperature of DPPC bilayers without peptide added is around 41 °C the

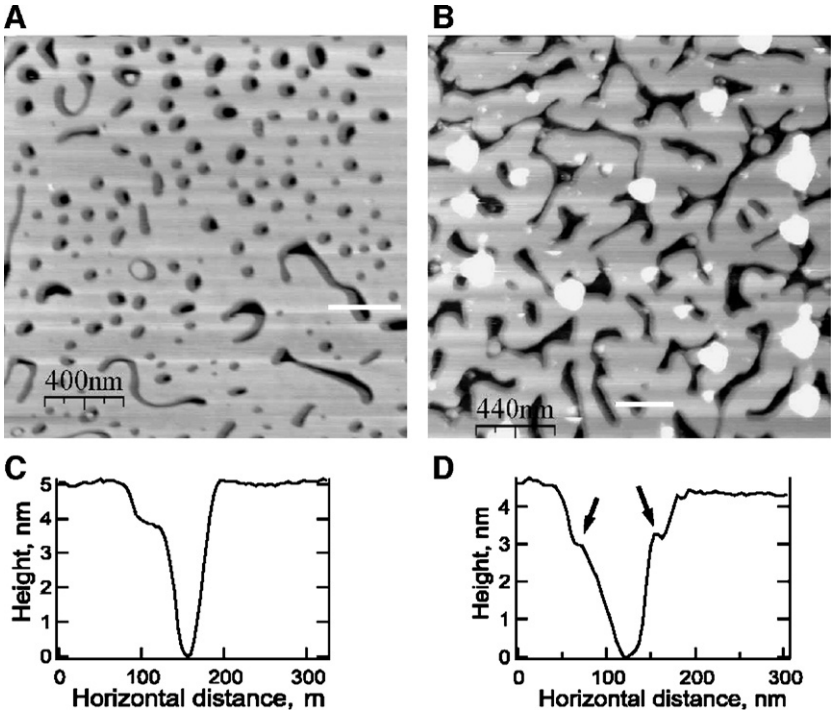

Fig. 3. AFM images of gel DPPC membranes supported on mica in the presence of alamethicin at different concentrations. (A) Height image (2×2 μm scan size) of 1 mol% alamethicin in a gel DPPC membrane. Selected section of the same sample as in Fig. 2A, but with smaller scan range. Dark regions represent the mica surface whereas coloured regions represent the lipid membranes. (B) Height image (2.2×2.2 μm scan size) of 4 mol% alamethicin in gel DPPC membrane. Very bright regions correspond to the particles of great height which are most probably pieces of titanium left after sample sonification. (C) and (D) are the cross-section height profiles along white marker lines extracted across selected alamethicin induced transmembrane defects in the figures A and B, respectively. Black arrows point to stepwise changes in the thickness of the gel DPPC membrane close to the peptide hole. Measured height differences correlate well with height difference between the thickness of a DPPC membrane in gel and fluid phase.

alamethicin-containing membrane will be in the gel phase at room temperature. The height of the shells close to the alamethicin induced holes corresponds to the thickness of fluid DPPC membranes [47]. Hence these are strong indications that these shells around the peptide induced holes are nanoscopic fluid phase lipid domains, spontaneously formed to reduce the structural mismatch. The length of alamethicin helices is about 3.5 nm which is significantly less than the thickness of DPPC membranes in the gel state. In order to reduce the unfavorite interactions at the peptide-lipid membrane interface between the DPPC hydrophobic chains and water, phospholipid molecules near alamethicin tend to exist in the fluid phase with reduced membrane thickness rather than in the gel phase with stretched hydrophobic chains.

Increasing the alamethicin concentration in DPPC bilayers up to 4 mol%, the peptide no longer forms circularly shaped defects but rather such with an elongated, branched, and irregular shape (Fig. 3B). Quite remarkable, the height reduction in the membrane close to alamethicin induced holes are also detected at this fourfold higher peptide concentration, as clearly revealed by the height profile (Fig. 3D). These findings demonstrate the similarity in the behaviour of membranes with different peptide concentration.

In Fig. 4 height and phase contrast images of a DPPC membrane containing 1 mol% alamethicin are presented. Again both images were simultaneously recorded in the tapping mode. The phase image clearly reveals some sites close to the holes with a bright contrast. This feature is also illustrated by the phase profile in Fig. 4D. This phase delay in the AFM tip vibrations indicates that the membrane surface close to the peptide induced hole is softer than the undisturbed lipid membrane. As mentioned in Materials and methods, such phase images have to be interpreted with care. Since we found the increase in the phase shift only close to the defects caused by peptides but not close to defects in pure membranes, we concluded that the shifts originate from the influence of the peptides on the mechanical properties of the membrane. Other contributions, e.g. from adhesion, cannot be ruled out completely. It is clear, however, that the presence of peptides at the inface of defects alters the phase image. Here, we favor the interpretation of membrane softening caused by peptides. Such softening of the gel phase DPPC bilayer close to the peptide aggregates shows the noticeable effect of alamethicin on the local compressibility of the membrane. This is again an indication of the DPPC molecules near alamethicin to exist in an altered physical state close to the transition range rather than in the gel phase that one expects at room temperature. The peptide induced softening of the lipid membrane close to the holes is in conformity with Monte Carlo simulations studies [23] which revealed increased fluctuations of the lipid phase near the peptide clusters. Larger fluctuations correspond to a higher compressibility and are expected in the phase transition regime. In the calorimetric measurements in Fig. 6 it is shown that the presence of the peptides lowers melting points (see below).

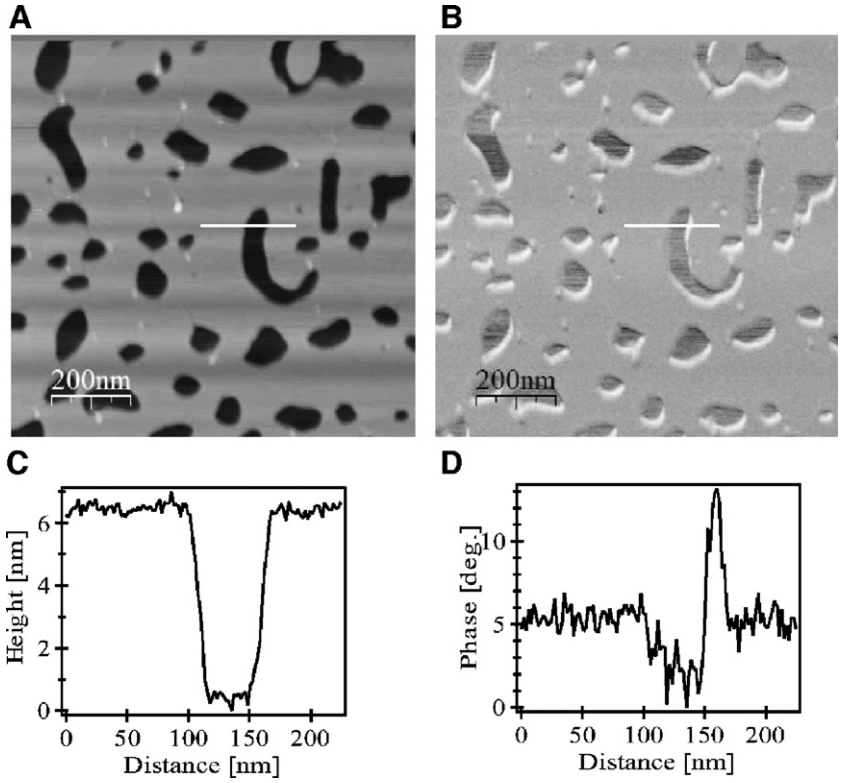

Fig. 4. Atomic force microscopy scans of gel DPPC lipid membrane with 1 mol% of alamethicin supported on mica. (A) Height and (B) phase images, respectively, from the 1 × 1 μm scan of the selected area from the Fig. 2D. The white line in both images depicts the cross-section height (C) and phase (D) profiles. Brighter areas close to peptide induced membrane defects depict greater phase shifts in AFM tip vibrations as can be seen also in phase cross-section plot (D).

Although the height image (Fig. 4A) as well as the height profile (Fig. 4C) do not reveal obvious changes in the membrane thickness near the peptide clusters, this feature is clearly present in other alamethicin/DPPC samples (Fig. 3). The slightly different appearance of identical sample preparations is likely due to small temperature variations between the different experiments because the atomic force microscopes were not provided with a temperature control. Obviously, in the example shown in Fig. 4 the lipid, as judged from the membrane thickness, is still in the gel phase but there exist already enhanced fluctuations between the two states as expected in the phase transition regime. For this reason there exist regions near the peptide clusters in which the compressibility of the membrane is enhanced, leading to the more detailed phase image.

In order to evaluate the hole sizes as induced by alamethicin in gel phase DPPC bilayers one can argue in terms of an "aggregation number", i.e., the number of peptides in the cluster around a hole filled with water. Measuring the length of the inner perimeter of every hole in the DPPC bilayers shown in Fig. 3A and B, we recorded the number of pores exhibiting a certain perimeter length. Assuming the peptide-to-peptide distance to equal ~11 Å [48,10], it is possible to estimate the number of peptides that form a hole by dividing the perimeter of the hole by the peptide-to-peptide distance mentioned above. In doing so we obtained a distribution of aggregation numbers shown by the histograms in Fig. 5A and B which are plotted for DPPC bilayer samples containing 1 and 4 mol% of alamethicin,

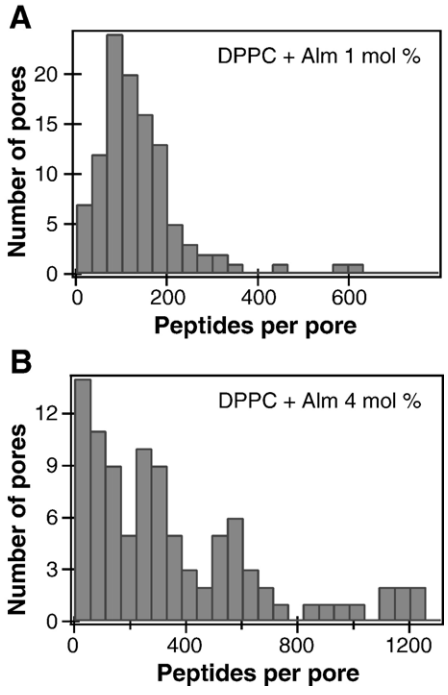

Fig. 5. (A) and (B) are histograms of distribution of peptide aggregation number per pore calculated for DPPC membranes with 1 and 4 mol% of alamethicin from AFM height images Fig. 3A and B, respectively. The number of peptides per pore was obtained by dividing the measured pore perimeter by the known peptide-to-peptide distance of ~11 Å known from literature.

respectively. From the histograms we obtained a ratio 1:3 for the total numbers of aggregated alamethicin molecules in membranes with 1 mol% and 4 mol% peptide concentrations, respectively. This ratio is larger than the 1:4 concentration ratio, probably, at least in parts, due to the experimental limitations. Height reductions with an area smaller than ~100 nm^2 were not taken into account, since the used AFM tips had a radius of curvature of about 10 nm. Peptide-induced holes, with dimensions smaller than the characteristic size of the AFM tip, could indeed be detected in height images, however, on such events the AFM tip could not reach the bottom of the hole, namely the mica surface. Therefore, the hole perimeter can only be estimated from the height images.

3.2. Differential scanning calorimetry

Excess heat capacity profiles (further on called "c_P-profiles") of large unilamellar vesicle (LUV) suspensions from DPPC and DMPC with different amounts of alamethicin added are displayed in Fig. 6A and B. For a clear data representation, plots of different alamethicin content were shifted along the heat capacity axis using a constant offset.

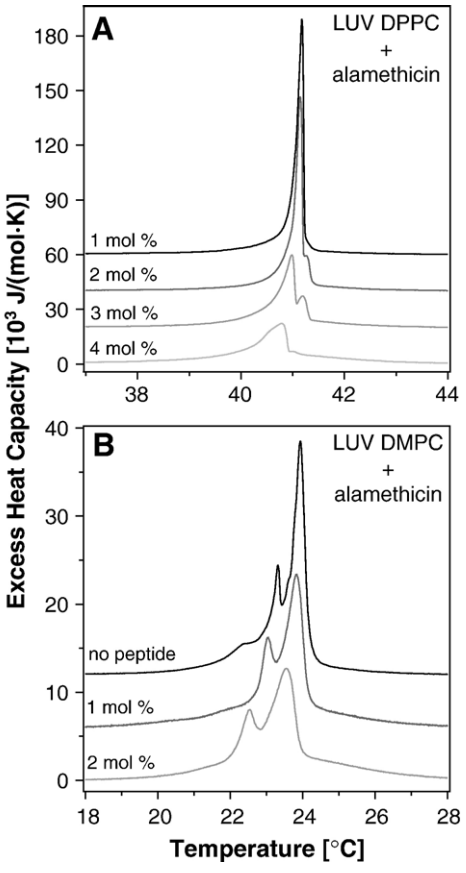

Fig. 6. Alamethicin in phosphocholine lipid membranes. (A) Heat capacity profiles of alamethicin in DPPC large unilamellar vesicles with 1, 2, 3 and 4 mol % of peptide. (B) Heat capacity profiles of alamethicin in DMPC large unilamellar vesicles with 0, 1 and 2 mol% of peptide. In all DSC-scans addition of alamethicin results in a minor shift to lower temperatures and in a broadening of the main transition peak. For a better data representation curves were shifted for a constant offset along the heat capacity axis.

Table 1
Melting temperatures T_m (°C) and enthalpy changes ΔH (kJ/mol) determined from c_P-profiles of alamethicin containing membranes shown in Fig. 6

Peptide content	DPPC		DMPC	
	T_m	ΔH	T_m	ΔH
0.0 mol%	41.6 [a]	39.3 [a]	23.6	22.2
1.0 mol%	41.18	34.8	23.4	22.5
2.0 mol%	41.17	34.6	22.9	23.1
3.0 mol%	40.98	29.7	–	–
4.0 mol%	40.79	32.4	–	–

[a] Values are taken from [47].

The heat capacity curve of the pure DPPC vesicles normally displays a maximum at ~41.6 °C, which is often called the main phase transition temperature, T_m. In the c_P-profiles shown in Fig. 6A, T_m and the shape of the transition peak are increasingly affected with the concentration of alamethicin within the DPPC membranes. This finding is also demonstrated by the T_m values listed in Table 1. The presence of peptide is reflected in those heat capacity profiles by a slight shift to lower temperatures accompanied by a small asymmetry at the low temperature wing and a transition peak broadening. However, at the highest measured peptide concentration of 4 mol%, the transition temperature is decreased by less than 1K only. The lipid melting enthalpy, ΔH, which is determined as the area under the heat capacity-versus-temperature profiles, decreases slightly when the alamethicin concentration in the DPPC vesicles increases up to 3 mol%. A similarly small influence of alamethicin on the c_P-profiles of DMPC vesicles was also observed (Fig. 6B). With DMPC membranes, however, ΔH increases slightly with alamethicin content. A change in the transition enthalpy of the DMPC system may, however, be caused by increasing uncertainty to accurately determine the base line.

In c_P-profiles of DPPC suspensions with alamethicin added one can also observe that, at 2 mol% of peptide, a small second peak appears at the high temperature slope of the main transition peak. It is more developed in the c_P-profile for 3 mol% of peptide but almost disappears with further increasing alamethicin content. The heat capacity profile of pure DPPC LUVs normally does not show up a splitting of the transition peak. However, in the case of extruded DMPC vesicles this feature exists (see Fig. 6B) and it is not noticeably affected by the presence of alamethicin. The splitting of the peak in c_P-profiles of pure DMPC LUV suspensions is believed to be related to changes of the vesicle geometry in the lipid melting regime, by analogy to a transition between lipid vesicles and a bilayer network during lipid phase transition of DMPG dispersions, as detected in electron microscopy experiments [49]. Probably, such appearance of an additional peak in c_P-profiles of alamethicin containing DPPC membranes reflects morphological changes of free lipid vesicles in solution, similar to the behaviour of DMPG vesicles [49]. This effect requires further investigations.

Heat capacity profiles for melittin containing multilamellar vesicles from DPPC and DMPC are displayed in Fig. 7. These vesicles do not show the splitting as observes with the LUVs.

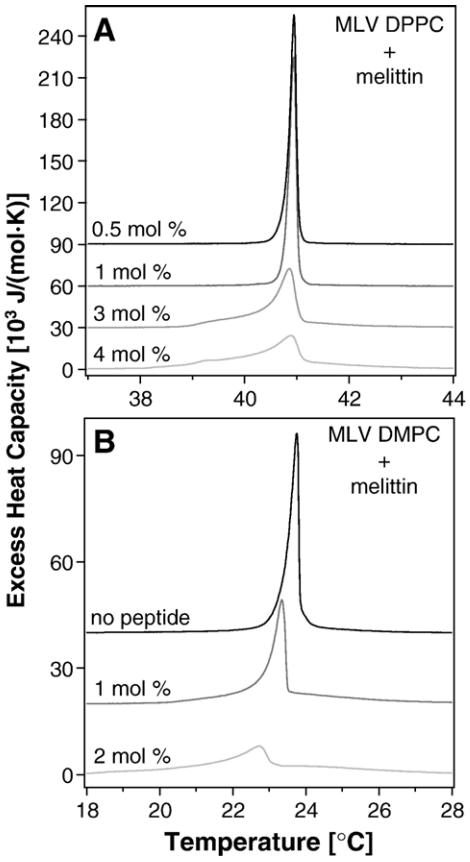

Fig. 7. Melittin in phosphocholine lipid membranes. (A) Heat capacity profiles of melittin-containing DPPC multilamellar vesicles with 0.5, 1, 3 and 4 mol% of peptide. (B) Heat capacity profiles of melittin in DMPC multilamellar vesicles with 0, 1 and 2 mol% of peptide. When melittin is added the phase transition temperature tends to decrease accentuating the low-temperature shoulder which becomes more pronounced when the melittin concentration is increased. For a better data representation curves were shifted for a constant offset along the heat capacity axis.

When melittin is added the phase transition temperature tends to decrease (Table 1). Again, however, the reduction of T_m with peptide content is small. More evident is the low-temperature shoulder in the c_P-profiles which becomes more pronounced when the melittin concentration is increased Fig. 7. Similar to alamethicin, melittin causes only small variations in the enthalpy changes ΔH at the chain melting temperature (Table 1).

4. Discussion and conclusions

Atomic force microscopy offers a valuable tool to visualize the spatial organization of peptide defects in membranes. For alamethicin containing bilayers we found that the peptide induces holes in gel state DPPC membranes, the hole structure depending on the peptide concentration. Since in the literature [6,7] pores are usually described as being very small we loosely refer to these holes as 'defects'. However, we have no evidence that the principle features of the peptide pores and our defects are different. An increase of alamethicin content up to 4 mol% in DPPC bilayers leads to the formation of bigger and more irregularly shaped transmembrane defects in comparison to the four times lower peptide concentration, at which alamethicin aggregates preferentially into smaller and almost circularly shaped holes. Such pore formation dependence upon the peptide content in membranes fits well to the commonly accepted barrel-stave model of alamethicin pores, in which multilevel conductance of alamethicin channels is assigned to a varying number of peptide molecules participating in the pore formation [13–17]. From calculations of pore perimeters in AFM height images (see Fig. 5A and B) we found that, at higher concentrations, alamethicin forms holes with a greater number of aggregated peptide molecules per pore. For 1 mol% of alamethicin the peptide aggregation number varies from 30 to 300 alamethicin molecules per hole with a maximum in the size distribution around 80, while at 4 mol% of alamethicin in DPPC membranes the number of peptide molecules forming a single aqueous defect can reach a value of up to 1200. However, such large numbers of alamethicin molecules, aggregated into a transmembrane hole, is not characteristic for alamethicin. For example, it was shown previously by neutron-scattering experiments [10] that in DLPC membranes pores are made of 8–9 monomers, with a water pore diameter of ~18 Å and with an effective outside diameter of ~40 Å. In diphytanoyl phosphatidylcholine membranes, the pores are made of n ~ 11 peptide molecules, with a water pore ~26 Å in diameter and with an effective outside diameter of ~50 Å [10]. On the other hand, it was suggested that a barrel-stave model with a water pore greater than 3.0 nm in diameter would consist of a bundle of 12 or more peptide helices, which is most likely unstable against shape deformation [50]. The observation of a wide distribution of the alamethicin aggregation number in our AFM experiments may suggest an effect of the mica surface on which the membranes were spread during the experiment. Contact with the mica crystal surface may stabilize alamethicin pores and holes. It is known that the direct contact of a membrane with mica can alter the occurrence of ripple structures in pure lipid membranes [35]. Therefore an influence of the mica on the present results cannot completely be ruled out. Additional experiments of multilayered membranes, in which the influence of the supporting surface is reduced, may be performed in future, in order to study this phenomenon in more detail. However, the formation of big pores by alamethicin molecules may be the native property of this peptide related to its antibiotic action. Alamethicin aggregates, consisting of a large number of peptide molecules, are difficult to detect utilizing neutron-scattering, while atomic force microscopy provides a possibility to inspect those peptide pores. However, pores with a number of peptide molecules smaller than about 30 (diameter smaller than 10 nm) cannot be resolved with AFM techniques because of the finite radius of curvature of the tip.

In melittin-containing membranes at 1 mol% peptide concentration transmembrane pores are formed in both DPPC and DLPC mica supported bilayers. Since DPPC membranes are in the gel phase at room temperature and DLPC membranes in the fluid phase, we conclude that the capability of melittin to form transmembrane defects does not depend on the state of the mica supported bilayer. The shape of the defects in both phases, however, is different. In DPPC bilayers melittin molecules form

elongated line-like structures, likely reflecting the high degree of ordering of the lipid matrix in the gel phase (similar structures were found for gramicidin A in the gel phase, [23]). In DLPC membranes melittin molecules aggregate to a highly disordered branched net of pores, in conformity with the less ordered fluid phase of the lipid membrane.

Another important result of this study of peptide-containing lipid membranes is the existence of nanoscopic domains of lower height in close vicinity to the peptide induced pores. In AFM images of the gel DPPC bilayers with alamethicin and also with melittin we found local height depressions close to the peptide pores. The height in these areas correspond to the thickness of DPPC membranes in the fluid phase [47]. This led us to the conclusion that, in a gel lipid membrane, the peptide induces melting of the surrounding lipids. Because of this melting a hydrophobic mismatch around peptide molecules is reduced and hereby the free energy of the system is minimized. From an free energy point of view alamethicin helices with lengths of ~3.5 nm and a predominantly hydrophobic surface [6] in water, tend to be rather surrounded by a DPPC membrane in the fluid phase with its thickness of ~3.9 nm than by a DPPC membrane in the gel phase with its larger thickness of ~4.8 nm [47]. Such an influence of peptide aggregates on the thermodynamic state of contacting lipids was also demonstrated in Monte Carlo (MC) simulations of peptide containing membranes [23]. It has been shown by those studies that the fluctuations of the lipid state at fixed temperature are higher close to the peptide aggregates embedded into the gel lipid matrix, which means a higher probability to find lipid molecules in a fluid state. Melting of peptide coupled lipids occurs at lower temperatures than of phospholipid membrane without peptides added. This is reflected by the heat capacity profiles. c_P-profiles of alamethicin containing membranes, shown in this work, demonstrate a shift of the transition peak to lower temperatures as compared to pure membranes. With increase of peptide content the shift of c_P-profiles is also larger. Such trends in the measured heat capacity curves are linked to the melting of certain fractions of lipids at lower temperatures and to the formation of nanoscopic fluid lipid domains close to the peptide-induced defects which were detected in the AFM experiments. The presence of peptide molecules in the membrane, which have a hydrophobic length shorter than the chain length of the surrounding lipids in the gel state tend to reduce the energetic barrier for changing their state from gel to fluid.

In MC-simulations of gramicidin A containing membranes it has been previously demonstrated [23] that peptide induced shifts of c_P-profiles can be explained in terms of peptide aggregation in lipid membranes. It was shown that considerable shifts of the transition peak to lower or higher temperatures correspond to a preferential aggregation of the peptide either in the gel or the fluid phase, while the unchanged main transition temperature is attributed to the similar tendency for peptide aggregation in both phases. For melittin-containing membranes we found that the peptide induces a shift of the transition peak in heat capacity profiles similar to alamethicin. Applying the above mentioned analysis one can predict melittin clustering (associated with pore formation) in both gel and fluid lipid membranes. This is in agreement with the AFM images presented in this work for DPPC (gel) and DLPC (fluid) membranes containing 1 mol% of melittin. Melittin aggregation into the transmembrane pores was observed in both membranes. We demonstrated also that the structure of melittin pores depends on the thermodynamic state of the membrane. In the case of fluid DLPC bilayer, melittin develops a network of transmembrane pores of higher density and more disordered structure as compared to gel DPPC bilayers containing the same amount of peptide. Therefore the lytic power of melittin should depend on the thermodynamic state of the membrane.

Hence, the peptides in model and biological membranes can strongly affect the local state of the system, and the effect of the peptide may also depend on the overall state of the membrane. Peptides like alamethicin tend to increase the permeability of biological membranes not only by forming water pores, but also by shifting the surrounding bilayer to more disordered states which are more permeable for small molecules. In turn, the state of the membrane can be a regulating factor of the action of antibiotic peptides like melittin, influencing their capability to form transmembrane pores.

Acknowledgements

We are indebted to Dr. T. Schäffer, University of Münster, for introducing one of us (V.O.) into atomic force microscopy and to Prof. T. Bjørnholm for generously making the equipment of the Nano-Science Center at the University of Copenhagen available for this study. Thanks are also due to Dr. M. Konrad, MPI for Biophysical Chemistry in Göttingen, for the synthesis of peptides. Financial support from the graduate school “Neuronal Signalling and Cellular Biophysics”, Georg-August-University of Göttingen, is also gratefully acknowledged.

References

[1] G. Spach, H. Duclohier, G. Molle, J.M. Valleton, Structure and supramolecular architecture of membrane channel-forming peptides, Biochimie 71 (1) (1989) 11–21.
[2] Y. Shai, Mechanism of the binding, insertion and destabilization of phospholipid bilayer membranes by k-helical antimicrobial and cell non-selective membrane lytic peptides, Biochim. Biophys. Acta 1462 (1999) 55–70.
[3] J.I. Kourie, A.A. Shorthouse, Properties of cytotoxic peptide-formed ion channels, Am. J. Physiol.: Cell Physiol. 278 (6) (2000) C1063–C1087.
[4] D.S. Cafiso, Alamethicin: a peptide model for voltage gating and protein–membrane interactions, Annu. Rev. Biophys. Biomol. Struct. 23 (1994) 141–165.
[5] C.E. Dempsey, The actions of melittin on membranes, Biochim. Biophys. Acta 1031 (2) (1990) 143–161.
[6] R.O. Fox, F.M. Richards, A voltage gated ion channel inferred from the crystal structure of alamethicin at 1.5 å resolution, Nature 300 (1982) 325–330.
[7] R.B. Gennis, Biomembranes, Springer, 1989, pp. 325–330.
[8] T. Terwilliger, L. Weissman, D. Eisenberg, The structure of melittin in the form I crystals and its implication for melittin’s lytic and surface activities, Biophys. J. 37 (1) (1982) 353–361.
[9] K. He, S. Ludtke, W. Heller, H. Huang, Mechanism of alamethicin insertion into lipid bilayers, Biophys. J. 71 (5) (1996) 2669–2679.
[10] K. He, S. Ludtke, D. Worcester, H. Huang, Neutron scattering in the plane

of membranes: structure of alamethicin pores, Biophys. J. 70 (6) (1996) 2659–2666.
[11] M.J. Zuckermann, T. Heimburg, Insertion and pore formation driven by adsorption of proteins onto lipid bilayer membrane–water interfaces, Biophys. J. 81 (5) (2001) 2458–2472.
[12] F.-Y. Chen, M.-T. Lee, H.W. Huang, Sigmoidal concentration dependence of antimicrobial peptide activities: a case study on alamethicin, Biophys. J. 82 (2) (2002) 908–914.
[13] J. Hall, I. Vodyanoy, T. Balasubramanian, G.R. Marshall, Alamethicin. A rich model for channel behavior, Biophys. J. 45 (1) (1984) 233–247.
[14] H. Duclohier, G. Molle, J. Dugast, G. Spach, Prolines are not essential residues in the "barrel-stave" model for ion channels induced by alamethicin analogues, Biophys. J. 63 (3) (1992) 868–873.
[15] D. Laver, The barrel-stave model as applied to alamethicin and its analogs reevaluated, Biophys. J. 66 (2 Pt. 1) (1994) 355–359.
[16] R. Cantor, Size distribution of barrel-stave aggregates of membrane peptides: influence of the bilayer lateral pressure profile, Biophys. J. 82 (5) (2002) 2520–2525.
[17] H. Duclohier, H. Wróblewski, Voltage-dependent pore formation and antimicrobial activity by alamethicin and analogues, J. Membr. Biol. 184 (1) (2001) 1–12.
[18] M. Eisenberg, J. Hal, C. Mead, The nature of the voltage-dependent conductance induced by alamethicin in black lipid membranes, J. Membr. Biol. 14 (1) (1973) 143–176.
[19] W. Hanke, G. Boheim, The lowest conductance state of the alamethicin pore, Biochim. Biophys. Acta 596 (3) (1980) 456–462.
[20] S.L. Keller, S.M. Bezrukov, S.M. Gruner, M.W. Tate, I. Vodyanoy, V.A. Parsegian, Probability of alamethicin conductance states varies with nonlamellar tendency of bilayer phospholipids, Biophys. J. 65 (1993) 23–27.
[21] R. Taylor, R. de Levie, "Reversed" alamethicin conductance in lipid bilayers, Biophys. J. 59 (4) (1991) 873–879.
[22] V.P. Ivanova, T. Heimburg, Histogram method to obtain heat capacities in lipid monolayers, curved bilayers, and membranes containing peptides, Phys. Rev., E 63 (2001) 1914–1925.
[23] V.P. Ivanova, I.M. Makarov, T.E. Schäffer, T. Heimburg, Analyzing heat capacity profiles of peptide-containing membranes: cluster formation of gramicidin A, Biophys. J. 84 (2003) 2427–2439.
[24] T.B. Pedersen, T. Kaasgaard, M. Jensen, S. Frokjaer, O.G. Mouritsen, K. Jørgensen, Phase behavior and nanoscale structure of phospholipid membranes incorporated with acylated C14-peptides, Biophys. J. 89 (4) (2005) 2494–2503.
[25] T. Heimburg, R.L. Biltonen, A Monte Carlo simulation study of protein-induced heat capacity changes, Biophys. J. 70 (1996) 84–96.
[26] Y.P. Zhang, R.N. Lewis, R.S. Hodges, R.N. McElhaney, Peptide models of helical hydrophobic transmembrane segments of membrane proteins. 2. Differential scanning calorimetric and FTIR spectroscopic studies of the interaction of Ac-K2-(LA)12-K2-amide with phosphatidylcholine bilayers, Biochemistry 34 (7) (1995) 2362–2371.
[27] O.G. Mouritsen, M. Bloom, Models of lipid–protein interactions in membranes, Annu. Rev. Biophys. Biomol. Struct. 22 (1993) 145–171.
[28] M.Ø. Jensen, O.G. Mouritsen, Lipids do influence protein function—the hydrophobic matching hypothesis revisited, Biochim. Biophys. Acta 1666 (2004) 205–226.
[29] P. Hansma, J. Cleveland, M. Radmacher, D. Walters, P. Hillner, M. Bezanilla, M. Fritz, D. Vie, H. Hansma, C. Parter, J. Massie, L. Fukunaga, J. Gurley, V. Elings, Tapping mode atomic force microscopy in liquids, Appl. Phys. Lett. 64 (13) (1994) 1738–1740.
[30] A. Janshoff, C. Steinem, Scanning force microscopy of artificial membranes, ChemBioChem 2 (11) (2001) 798–808.
[31] S.D. Connell, D.A. Smith, The atomic force microscope as a tool for studying phase separation in lipid membranes, Mol. Membr. Biol. 23 (1) (2006) 17–28.
[32] B. de Kruijff, J.A. Killian, D.N. Ganchev, H.A. Rinia, E. Sparr, Striated domains: self-organizing ordered assemblies of transmembrane alpha-helical peptides and lipids in bilayers, Biol. Chem. 387 (3) (2006) 235–241 (doi.org/10.1515/BC.2006.031).
[33] L.K. Nielsen, A. Vishnyakov, K. Jørgensen, T. Bjørnholm, O.G. Mouritsen, Nanometre-scale structure of fluid lipid membranes, J. Phys., Condens. Matter 12 (8A) (2000) A309–A314.
[34] F. Tokumasu, A.J. Jin, G.W. Feigenson, J.A. Dvorak, Nanoscopic lipid domain dynamics revealed by atomic force microscopy, Biophys. J. 84 (2003) 2609–2618.
[35] C. Leidy, T. Kaasgaard, J.H. Crowe, O.G. Mouritsen, K. Jørgensen, Ripples and the formation of anisotropic lipid domains: imaging two-component supported double bilayers by atomic force microscopy, Biophys. J. 83 (2002) 2625–2633.
[36] H.A. Rinia, B. de Kruiji, Imaging domains in model membranes with atomic force microscopy, FEBS Lett. 504 (2001) 194–199.
[37] T. Kaasgaard, C. Leidy, H. Crowe, O.G. Mouritsen, K. Jørgensen, Temperature-controlled structure and kinetics of ripple phases in one- and two-component supported lipid bilayers, Biophys. J. 85 (1) (2003) 350–360.
[38] J. Mou, D. Czajkowsky, Z. Shao, Gramicidin A aggregation in supported gel state phosphatidylcholine bilayers, Biochemistry 35 (10) (1996) 3222–3226.
[39] V.V. Plotnikov, J.M. Brandts, L.-N. Lin, J.F. Brandts, A new ultrasensitive scanning calorimeter, Anal. Biochem. 250 (2) (1997) 237–244.
[40] R.C. MacDonald, R.I. MacDonald, B.P.M. Menco, K. Takeshita, N.K. Subbarao, L. rong Hu, Small-volume extrusion apparatus for preparation of large, unilamellar vesicles, Biochim. Biophys. Acta 1061 (1991) 297–303.
[41] G. Binnig, C. Quate, C. Gerber, Atomic force microscope, Phys. Rev. Lett. 56 (9) (1986) 930–933.
[42] Z. Shao, J. Yang, Progress in high resolution atomic force microscopy in biology, Q. Rev. Biophys. 28 (2) (1995) 195–251.
[43] J.F. Nagle, Theory of the main lipid bilayer phase transition, Annu. Rev. Phys. Chem. 31 (1980) 157–195.
[44] L. Makowski, J. Li, Topics in Molecular and structural Biology: Biomembrane Structure and Function., Weinheim, 1984, Ch. X-ray diffraction and electron microscope studies of the molecular structure of biological membranes., pp. 43–166.
[45] L.K. Tamm, H.M. McConnell, Supported phospholipid bilayers, Biophys. J. 47 (1) (1985) 105–113.
[46] J. Mou, J. Yang, Z. Shao, Tris(hydroxymethyl)aminomethane (C4H11NO3) induced a ripple phase in supported unilamellar phospholipid bilayers, Biochemistry 33 (15) (1994) 4439–4443.
[47] T. Heimburg, Mechanical aspects of membrane thermodynamics. Estimation of the mechanical properties of lipid membranes close to the chain melting transition from calorimetry, Biochim. Biophys. Acta 1415 (1998) 147–162.
[48] A. Spaar, C. Münster, T. Salditt, Conformation of peptides in lipid membranes studied by X-ray grazing incidence scattering, Biophys. J. 87 (2004) 396–407.
[49] M.F. Schneider, D. Marsh, W. Jahn, B. Kloesgen, T. Heimburg, Network formation of lipid membranes: triggering structural transitions by chain melting, Proc. Natl. Acad. Sci. U. S. A. 96 (25) (1999) 14312–14317.
[50] L. Yang, T.A. Harroun, T.M. Weiss, L. Ding, H.W. Huang, Barrel-stave model or toroidal model? A case study on melittin pores, Biophys. J. 81 (3) (2001) 1475–1485.